BRITISH GEOLOGICAL SURVEY

Natural Environmental Research Council

TECHNICAL REPORT
Hydrogeology Series

Technical Report WD/93/24R

Laboratory determination of wettability, capillary pressure curves, pore entry pressure and relative permeabilities in immiscible phase-brine systems.

J P Bloomfield
May 1993

Abstract.

Methods for the laboratory determination of wettability, 'capillary pressure' curves, pore entry pressures and relative permeability in immiscible phase-brine systems are briefly reviewed.

It is noted that measurement of wettability should be an integral part of the study of immiscible phase-brine systems. The measurement of contact angles in immiscible phase-brine-rock systems is not thought to be appropriate in characterising the wettability of geological materials, and comparative, phenomenological, tests such as the Amott test are believed to be more suitable (these latter tests are simple to perform and do not require sophisticated equipment).

Mercury Injection Capillary Pressure (MICP) tests are used to generate 'capillary pressure' curves. They are relatively rapid tests and can provide information on pore throat size distributions (the technique is currently available within the Aquifer Properties Laboratory of the Hydrogeological group). However, their use in predicting pore entry pressures in specific immiscible phase-brine-aquifer systems is untested. A more desirable approach would be to study the capillarity of the systems of interest, either using 'capillary pressure' cells (a lengthy experimental procedure), or through the use of centrifuge tests.

Relative permeabilities are obtained from waterflood susceptibility tests. Relative permeabilities are commonly cited at residual oil or water saturations, such data is obtained from basic waterflood tests, but relative permeabilities may be measured over a range of saturations using either steady-state or non-steady-state waterfloods, or by using centrifuge techniques.

Centrifuge techniques are a potentially powerful tool in the investigation of immiscible phase-brine-aquifer systems. Wettability, 'capillary pressure curves' (and hence pore entry pressures), and relative permeabilities (over the entire range of saturations) can be obtained from a single test.

Acknowledgements

I would like to thank Adrian Lawrence and Daren Gooddy for initial discussions concerning the properties of immiscible phase-brine systems. I would also like to thank Ann Williams and Daren Gooddy for reviewing various drafts of the report and Kate Horner for providing the original drawings for Figure 4.2.

Table of contents

1.0 Introduction

The aim of this report is to present a brief review of experimental techniques that may be used in the determination of wettability, 'capillary pressure' curves, pore entry pressures, and relative permeabilities in immiscible phase-brine-aquifer systems.

Section 2.0 begins the review by establishing a working definition of wettability. Two industry standard wettability measurement techniques are then described in Section 2.1.

Section 3.0 presents working definitions for 'capillary pressure' and pore entry pressure and discusses these with reference to a more rigorous definition of capillary pressure (given in Section A.1 of the Appendix). A range of standard experimental techniques used to obtain 'capillary pressure' curves and pore entry pressure are described in Section 3.1. Some problems associated with the interpretation of 'capillary pressure' curves are noted and discussed in this section.

Section 4.0 provides a qualitative description of the effect of contrary wettabilities on the relative permeability and residual saturations of three phase systems and discusses a number of working definitions of residual saturation. The use of waterflood tests in the determination of relative permeabilities at residual water and oil saturations is also discussed. Sections 4.1 and 4.2 outline two general classes of experimental measurement techniques employed in relative permeability determination. The merits of the respective techniques are noted.

The Appendix, Section A.1, presents rigorous definitions of surface tension, surface free energy and capillary pressure. It also establishes formal relationships between surface tension, capillary pressure and contact angles in simple three phase (solid-liquid-vapour, or solid-liquid-liquid[immiscible]) systems. In addition, Section A.2 of the Appendix gives details of some of the published solutions to the calculation of sample saturations in centrifuge tests, and Section A.3 is a brief description of the Buckley-Leverett displacement theory (applicable to relative permeability studies).

Throughout this note the two immiscible fluid phases may be any two immiscible fluids with contrary wetting characteristics, eg. water-oil, water and chlorinated solvent, water and air (the terms water and brine are used interchangeably throughout the text).

2.0 Working definition of wettability

The natural affinity of a fluid phase to coat a surface is known as wettability. In three phase systems the contrary wettabilities of each fluid phase play an important role in determining the pore entry pressure and relative permeability characteristics of the material. Hence an integral part of any three-phase study is the investigation of wetting preferences.

Wettability is controlled by surface processes at the fluid-solid and fluid-fluid interfaces. Consequently, wettability is a function of the contact angle of the fluids

with the solid surface, the surface free energies of the interfaces of the three phases (solid-fluid-fluid), and the pressure drop across the fluid-fluid interface in the system, see Appendix A.1 for details.

The physical expression of the relationship between contact angle and wettability is illustrated schematically in Figure 1.1. A flat, water wet, mineral plate will cause oil on its surface to ball up, such that the contact angle between the plate and the water is significantly less than 90°, and may approach 0° (Figure 1.1a). In contrast, if the plate is oil wet, oil will spread easily over the mineral to coat the surface, in this case the contact angle between the water and the plate will be >90° and will approach 180° (Figure 1.1b).

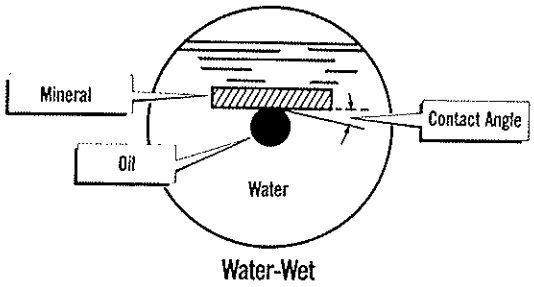

Figure 1.1a

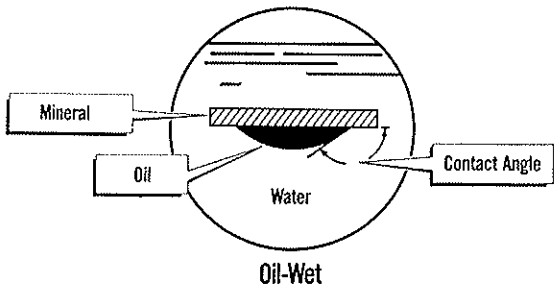

Figure 1.1b

Figure 1.1 *Illustration of the relationship between contact angles (measured through the aqueous phase) and the wetting characteristics of mineral plates in an oil-water-mineral system (from Core Laboratories course notes).*

In a relatively clean, coarse, sandstone the wettability to a given fluid may approximate to the idealized three phase system illustrated in Figure 1.1, so that it may have a wettability similar to that of the wettability of a quartz plate to the fluid under consideration. However, most rocks are highly heterogeneous and have complex mineralogies, and, consequently, generally unpredictable wetting characteristics. As a result standard methods for measuring wettability, ie. measuring contact angles in mineral-fluid-fluid systems, may not adequately predict the wetting characteristics of a given rock.

Instead phenomenological investigations of rock wetting characteristics in two immiscible fluid phase systems need to be undertaken. Such tests are described in Section 2.1. The problem with using phenomenological tests is that the results are difficult to interpret in terms of established wetting theory. In addition, the phenomenological 'wetting indices' that they produce only have real significance when a number of observations on a range of rock-fluid-fluid systems have been obtained, and when the indices have been correlated with other, well constrained, empirical observations.

2.1 Measurement of wettability

A range of methods have been used to measure wettability, eg.

1. direct measurement of contact angles in simple solid-fluid-fluid systems,

2. the Amott test, a test to measure the spontaneous imbibition of two immiscible phases in rock-fluid-fluid systems and

3. pseudo 'capillary pressure' techniques.

Of these methods the two standard tests in the geological literature are the Amott test (an oil industry standard) and the USBM (United States Bureau of Mines standard) pseudo 'capillary pressure' technique. Details of a range of techniques for the direct measurement of contact angles in simple three phase systems are given in Adamson (1960), however, this type of technique is not detailed here as it is not considered useful in the investigation of mineralogically complex geological materials.

The following sections briefly describe the use of the Amott test and the USBM pseudo 'capillary pressure' techniques in defining wettability. Both techniques establish empirical wettability indices based on some ratio of the ability of a rock to imbibe the immiscible phase.

2.1.1 Amott test

The Amott test procedure is illustrated in Figure 2.1. The technique is based on the premise that a strongly wetting fluid will be spontaneously imbibed by a solid until the residual saturation of the non-wetting fluid is obtained. A (preserved) plug is drilled using a fluid comparable to the coring fluid (ie. if a water based mud was used during drilling then the plug should be cored with water) and then flushed and saturated with water to remove any gas. This establishes a residual oil saturation in the sample (see Section 4.0).

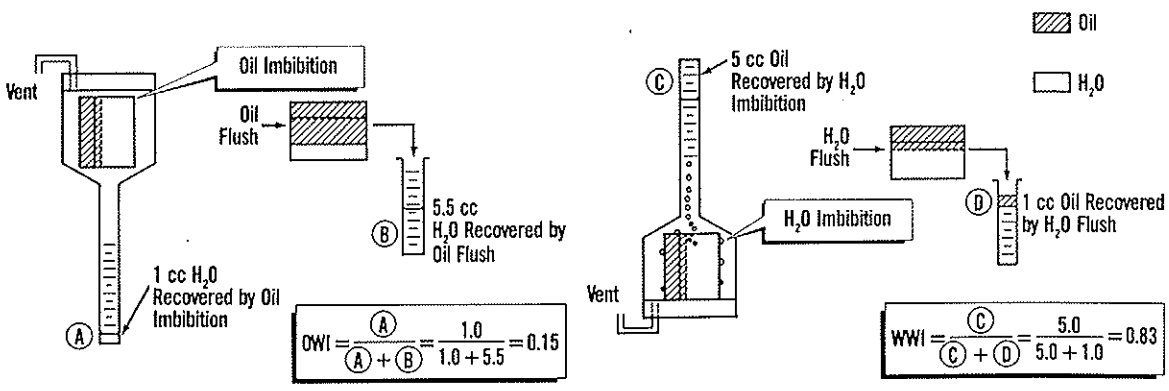

Figure 2.1 *Graphical illustration of the Amott test procedure, see text for details (from Core Laboratories course notes).*

The plug is then placed in an imbibition tube under oil, and water is displaced spontaneously by oil imbibition. Variation in the volume of displaced water with time will be observed. Once water has ceased to be displaced the total volume of displaced water, V_{wd}, is recorded. The core is removed from the flask and flushed with oil and the volume of water which is displaced is again monitored.

Once the volume of flushed water is constant the total volume of flushed water, V_{wf}, is recorded.The oil wet index is defined as,

$$\text{Oil wet index} = V_{wd} / (V_{wd} + V_{wf}) \qquad 2.1$$

The sample is then placed in the imbibition tube under water and oil displaced by spontaneous water imbibition. The final volume of displaced oil is measured, V_{od}. The core is taken out of the tube and flushed with water. The final volume of flushed oil, V_{of} is then measured.

The water wet index is defined as,

$$\text{Water wet index} = V_{od} / (V_{od} + V_{of}) \qquad 2.2$$

In each case an index of 1.0 indicates a strongly wetting fluid and an index of 0.0 indicates a strongly non-wetting fluid.

2.1.2 USBM wettability index

The USBM method of obtaining a 'wettability index' is a pseudo-'capillary pressure' technique (Donaldson et al. 1969) that compares the areas under 'capillary pressure' curves for two liquid phases. The method has been established using 'capillary pressure' curves obtained by centrifuging. This section is only concerned with the definition of the USBM 'wettability index' and does not give details of the experimental methods employed in obtaining the curves (the centrifuge technique is described in Section 3.1.3).

For an oil-water system the procedure is as follows. The sample to be tested is first saturated in brine before being spun under oil at high speed to reduce it to a residual water saturation (S_{wi}). The sample is then placed under brine and centrifuged at incrementally increasing speeds, hence increasing the pressure exerted on the sample. At each increment of spin speed the total volume of evolved oil is recorded. Centrifuge speeds and the volumes of evolved water are used to calculate a 'capillary pressure' and a partial brine saturation; this step is known as the brine drive.

Following this the sample is paced in oil and again centrifuged at incrementally increasing speeds. Now the oil displaces brine from the sample and again 'capillary pressure' and partial oil saturations are calculated for each incremental speed; this is known as the oil drive. 'Capillary pressure' curves are constructed, for both the water and oil drive stages, using the incremental 'capillary pressures' and partial sample saturations. Figure 2.2 (Donaldson et al. 1969) illustrates the brine and oil drive 'capillary pressure' curves obtained for typical water wet, oil wet, and neutral

systems. The figure also illustrates the reduction in partial brine saturation during initial spinning under oil to its residual brine saturation (shown as dashed lines in the figures). The USBM Wettability Index, W_i, is defined on the basis of the areas under the respective 'capillary pressure' curves as follows;

$$W_i = \text{Log}\ (A_1/A_2) \qquad 2.3$$

where A_2 is the area under the brine drive curve and A_1 is the area under the oil drive curve.

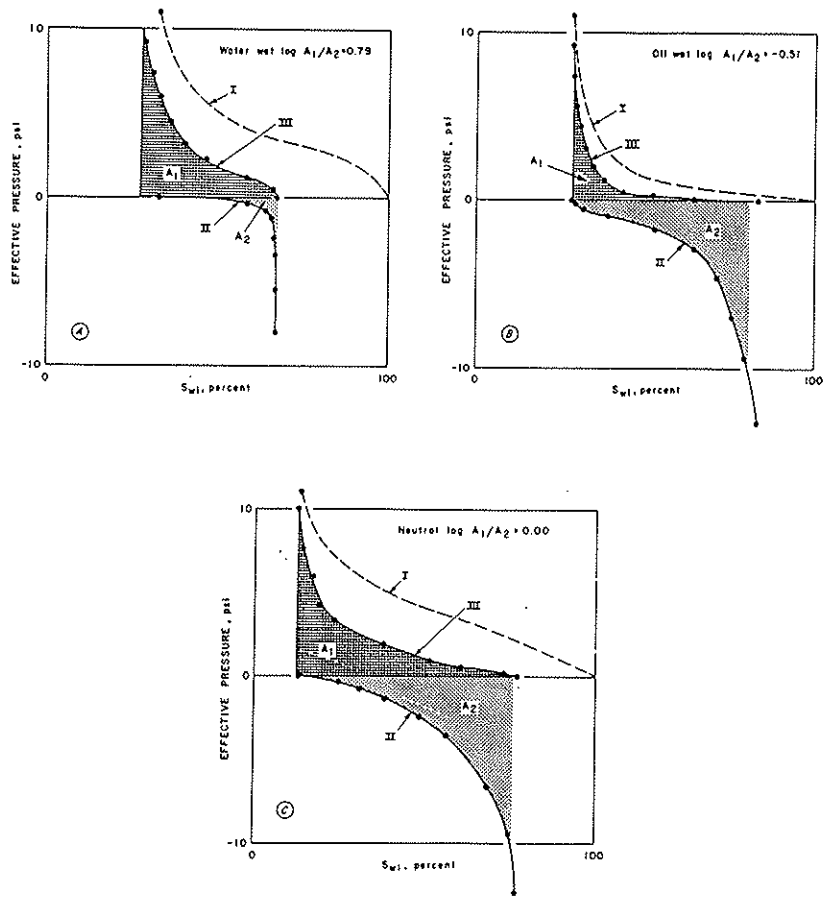

Figure 2.2 *Illustration of the effect of wettability on the form of brine drive and oil drive 'capillary pressure' curves, see text for details (from Donaldson et al. 1969).*

The Wettability Index, as defined in Eqn 2.3, is a function of the relative wetting tendencies of the fluids and of the pore size distributions that control the form of the 'capillary pressure' curves. In general, water wet systems may be expected to have larger areas under the oil drive curves than the brine drive curves, therefore, the Wettability Index for a water wet system should be positive. For an oil wet system the Wettability Index should be negative. Note that in the neutral case in Figure 2.2, even though the areas under the two curves are similar the two curves are not symmetrical. This is due to hysteresis effects, eg. order of wetting and trapping or pooling of immiscible phases.

3.0 Immiscible phase pore entry pressure

Before some techniques for measuring immiscible phase pore entry pressures are described it is necessary to establish working definitions for pore entry pressure and capillary pressure.

3.0.1 Working definition of pore entry pressure

Pore entry pressure is an inexact term. It may be used to describe the single valued pressure required to cause intrusion of a fluid into a single capillary, or group of identical capillaries, or it may be used to describe the limited pressure range over which significant fluid intrusion occurs in a rock mass with a complex pore geometry. In the former case of a capillary, or bundle of capillaries, the pore entry pressure is equivalent to the capillary pressure, $\Delta \mathbf{P}$, of Eqn A.1.5. However, in the latter case the pore entry pressure is not equivalent to the capillary pressure of Eqn A.1.5, but is a complex function of individual capillary pressure events within the rock mass.

Pore entry pressure may be obtained from phenomenological tests. A pair of typical drainage/wetting curves (applied pressure vs phase saturation) are illustrated in Figure 3.1 (drainage curves may be obtained by forcing air, under pressure, into a water wet, water saturated core). During drainage, sample saturation, S, is very close to unity over a finite range of applied pressures, p_c, however, when some critical value of applied pressure (nominally the pore entry pressure) is exceeded saturation decreases rapidly. It has been suggested (White et al. 1972) that any desaturation occurring prior to the critical applied pressure takes place in pore spaces exposed at the sample boundaries, and that the non-wetting phase (eg. air) cannot reach the interior of a sample until an interconnected network of channels have been desaturated. White et al. (1972) also suggested that the inflection point on the drainage curve, where dS/dp_c is at a maximum, corresponds to the highest saturation at which the non-wetting phase is interconnected, ie. at which non-wetting phase permeability exists.

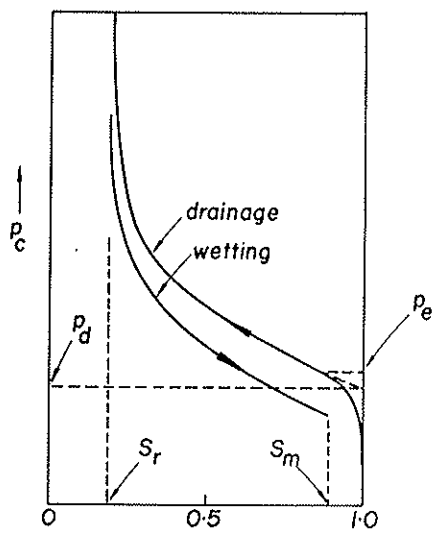

Figure 3.1 *Illustration of typical drainage and wetting curves plotted as applied pressure vs saturation. Note the hysteresis commonly observed between drainage and wetting, or imbibition curves.*

There is some ambiguity as to which point on the desaturation curve represents the critical value of applied pressure, or pore entry pressure. Petroleum scientists define a displacement pressure, p_d, as the pressure at which first desaturation on a drainage cycle occurs. For practical purposes they obtain p_d by extrapolating the curve to the ordinate (see Figure 3.1) where S is 1, but neglect that part of the measured data which is interpreted as being due to surface effects. Soil scientists define an 'air-entry pressure', p_e, as the pressure required force air through an initially water saturated sample (see Figure 3.1). Commonly the value of S at p_e is in the range 0.8 to 0.9.

3.0.2 Working definition of capillary pressure

Capillary pressure, ΔP, is defined rigorously in the Appendix (Section A.1.1, Eqn A.1.5), but is taken here to mean the pressure difference existing across an interface between two immiscible fluids (considered to be wetting and non-wetting), where the interface is constrained between solid surfaces.

In phenomenological pore entry pressure tests the applied pressure is equivalent to some average 'capillary pressure', which is in turn in balance with average surface tensions in the three phase system, and is also a function of the pore geometry (an average capillary, pore or pore throat radius). Plots such as that illustrated in Figure 3.1 are commonly referred to as capillary pressure curves, but because the pressure axis is not a true capillary pressure (as defined in Eqn A.1.5) these type of tests and curves will be referred to as 'capillary pressure' tests and curves.

A variety of factors influence the form of 'capillary pressure' curves obtained from phenomenological tests, eg. the relative wettability of the phases, sample saturation history, and rock texture/pore geometry. In addition, hysteresis can be observed in cyclic imbibition and drainage tests (Topp 1969). Hysteresis may be effected by the order of wetting of the solid phase in a three phase system.

3.1 Measurement techniques

'Capillary pressure' curves may be obtained by a number of techniques;

1. Mercury Injection Capillary Pressure (MICP) tests.
2. 'Capillary Pressure' cell tests.
3. A pseudo 'Capillary Pressure' centrifuge technique.

Each of these techniques are briefly described below.

3.1.1 Mercury Capillary Pressure Injection (MICP) tests

MICP tests use the forced imbibition of non-wetting mercury (mercury-silica contact angle is approximately 130°) into small plugs of rock material to obtain 'capillary pressure' curves. A detailed description of the technique, including notes on experimental errors, is given in Bloomfield et al. (1992).

Sample material (which may be either consolidated or unconsolidated) is placed in a penetrometer stem and sealed in a bell jar containing mercury; a vacuum is then pulled down. When a sufficient vacuum has been achieved the tip of the penetrometer stem is placed under the mercury and air slowly admitted into the bell jar causing mercury to flood into the stem of the penetrometer. The penetrometer stem is now primed with mercury, the sample surrounded by mercury, but the pore space within the sample under partial vacuum. The penetrometer is then removed from the mercury and air is again slowly admitted into the bell jar. The increasing air pressure acts on the free surface of the mercury at the tip of the penetrometer stem and may cause intrusion of mercury into the sample pores. Pressure in the bell jar is increased until atmospheric pressure is achieved.

The penetrometer stem is then removed from the bell jar, sealed into a high pressure hydrostatic cell, and is slowly pressurized to a maximum pressure of approximately 50,000 psi. The pressure acting on the free surface of the mercury column may again cause intrusion of mercury into the core.

During both the pressurization cycles pressure and the volume of intruded mercury are continually monitored and logged on a microcomputer. The volume of intruded mercury is proportional to the change in length of mercury column in the penetrometer stem, which is measured by a change in the capacitance of a sensing system.

Results of these tests are usually presented as cumulative intrusion vs pressure, or 'capillary pressure', curves and relative intrusion vs pressure histograms (an example of a typical plot is shown in Figure 3.2). The relative intrusion histograms are obtained from the slope of the 'capillary pressure' curves over a prescribed pressure interval (in Figure 3.2 the histogram is based on 20 divisions per decade of absolute pressure). These histograms are particularly useful in highlighting dominant pore entry pressures.

Figure 3.2 is calibrated along its upper x-axis for pore diameter (microns). These pore diameters have been calculated by rearranging Eqn A.1.7 for pore radius and by substituting values of interfacial tension for mercury-air surfaces, mercury contact angle (taken as 130°), and applied hydrostatic pressure. It is not clear how valid this procedure is because, as previously noted in Section 3.0, Eqn A.1.7 may only be rigorously applied to capillaries in simple three phase systems. Again it should be emphasised that the hydrostatic pressures applied during the test are only a function of some averaged capillary pressure within the sample. The predicted pore diameters have not been correlated with direct observations of pore structure, although it is commonly inferred that they represent pore throat diameters and not pore diameters.

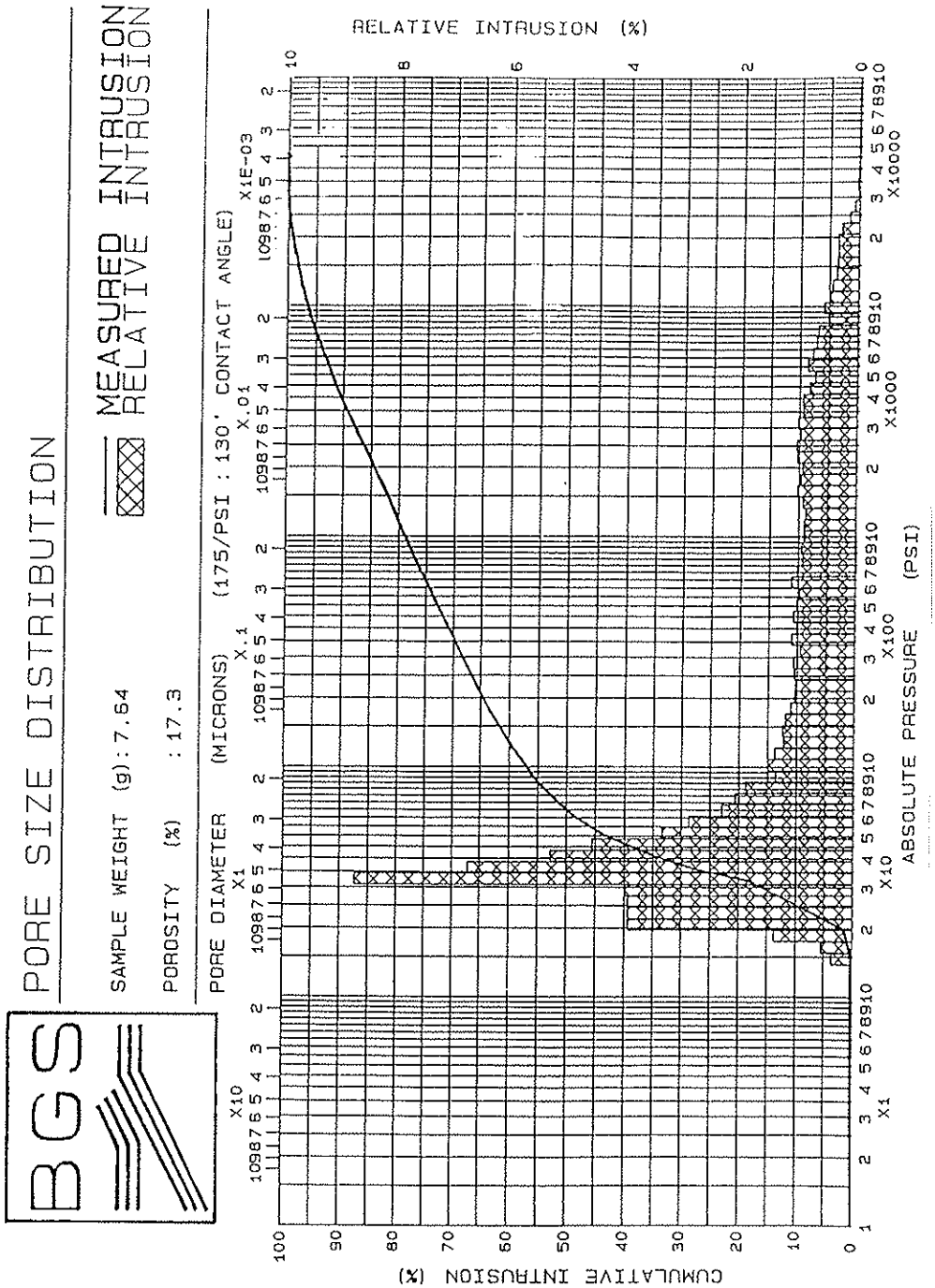

Figure 3.2 *A plot illustrating the output from a typical MICP test on a Permo-Triassic sandstone. The bold sigmoidal curve is the measured cummulative intrusion (percentage as indicated on the left hand axis) and the derrived histogram (see text for details) is the relative intrusion (percentage as indicated on the right hand axis). The plot may be interpreted as indicating a dominant pore throat diameter of approximately 5.5 microns in the sandstone.*

3.1.2 'Capillary Pressure' cell tests

'Capillary Pressure' cell tests are usually performed as drainage tests, where a pressurized gaseous phase displaces a saturant from cores via a porous plate at their base. However, a modification of the 'capillary pressure' cell tests permits forced drainage curves to be obtained for immiscible phase systems.

These tests require samples to be saturated in brine and placed on individual porous ceramic plates. The sample is then flooded under the immiscible phase which is pressurized (by compressed air at the free surface). The forced imbibition of the immiscible phase into the sample causes brine to be driven off through the under pressured porous plate and into a calibrated tube. The expelled volume of water is measured and used to calculate sample saturation. The immiscible phase pressure is then increased and the new volume of evolved water recorded.

A 'capillary pressure' curve for a forced drainage can be produced from the immiscible phase pressure/brine saturation data. Unlike the MICP tests where typically between 100 and 200 pressure/partial saturation observations are collected, 'capillary pressure' cell tests usually generate 5 or 6 data points. Consequently, it is not possible to obtain meaningful relative intrusion histograms and the immiscible phase pore entry pressure has to be obtained from the form of the poorly defined curves.

The 'capillary pressure' cell tests are relatively slow and may take of the order of three months to perform. It may take a couple of weeks for the volume of evolved water to stabilize at each of the pressure steps (a minimum of 5 or 6 steps is required to characterise the curve).

3.1.3 Use of a centrifuge to obtain pore entry pressure curves

A third method of obtaining 'capillary pressure' curves is by using a centrifuge, ie. the pseudo-capillary pressure technique. This method relies on established relationships between 'capillary pressures', local saturations along the length of a core, and average core saturation during spinning tests (Section A.2). 'Capillary pressure' curves may be obtained for brine-air systems by spinning saturated samples in air, or may be obtained for immiscible phase systems by spinning saturated samples while submerged in the second liquid phase.

Due to centrifugal forces, when a saturated core is spun at a constant angular speed a pressure gradient, and corresponding saturation gradient, is established along the core length. Since pressure at any point along the sample is proportional to the centrifuge speed, the pressure at the end of the sample nearest to the axis of rotation can be calculated if sample size and rotor size are known. Additionally, during centrifuging a volume of the saturant is expelled from the end of the sample furthest from the axis of rotation. Using the volume of expelled water a mean sample saturation can be calculated. Given the 'capillary pressure' and the average saturation of the sample, the saturation at the end of the sample nearest to the axis of rotation can be calculated (see Appendix, Section 2.0 on the centrifuge equation).

If the centrifuge speed is increased an additional volume of water may be evolved and a new capillary pressure and saturation can be calculated. This data can then be used to construct a 'capillary pressure' curve.

The centrifuge technique has a number of advantages over the other two 'capillary pressure' techniques. Unlike the 'capillary pressure' cell technique it is relatively fast and unlike the MICP tests it can be used to generate immiscible phase 'capillary pressure' curves or brine 'capillary pressure' curves in the presence of the second phase. The method requires a specialized centrifuge that permits the volume of evolved brine or oil to be measured during the course of a spinning cycle (eg. Beckman centrifuge). However, using such a centrifuge it should be possible in a single test, to obtain not only 'capillary pressure' curves but also to obtain immiscible phase pore entry pressure data, a Wettability Index (USBM method), the relative permeabilities of each of the phases (see Section 4.2) and information concerning residual phase saturations.

4.0 Relative permeability

Before relative permeability measurement techniques are described the concepts of residual and effective saturations are briefly discussed, and the influence of wettability on relative permeability and residual saturation are noted. Throughout the following section the two immiscible liquids are taken to be water (or brine) and oil but may be any two immiscible phases with contrary wetting characteristics.

4.0.1 Residual and effective saturations

As a working definition, residual saturation, S_r, is the saturation value for a given phase for which there is negligible change when applied pressure increases very rapidly. Residual saturation is commonly referred to as the irreducible saturation, or the minimum saturation. The term residual saturation is preferred to the terms irreducible or minimum saturation since the latter have physical implications which are not reasonable.

The physical meaning of residual saturation depends to a large extent on how saturation is measured. A number of workers have suggested that it represents a saturation value where films of the wetting phase on the solid surfaces are no longer interconnected, and that the wetting phase exists only as pendular rings at points of grain-grain contact. However, this view contradicts the observation that the wetting phase never becomes completely immobile as typical saturation curves are always asymptotic to a residual saturation value (eg. Figure 3.1).

Relative permeability is defined as the ratio of effective permeability to a base permeability. For oil-water systems the base permeability is usually taken to be the permeability of oil at the residual water saturation S_{rw}. The results of relative permeability tests are commonly presented as water-oil relative permeability curves, ie. plots of calculated permeabilities against measured saturations, two typical examples are shown in Figure 4.1. Relative permeabilities are strongly dependent on saturation history and hysteresis effects are common.

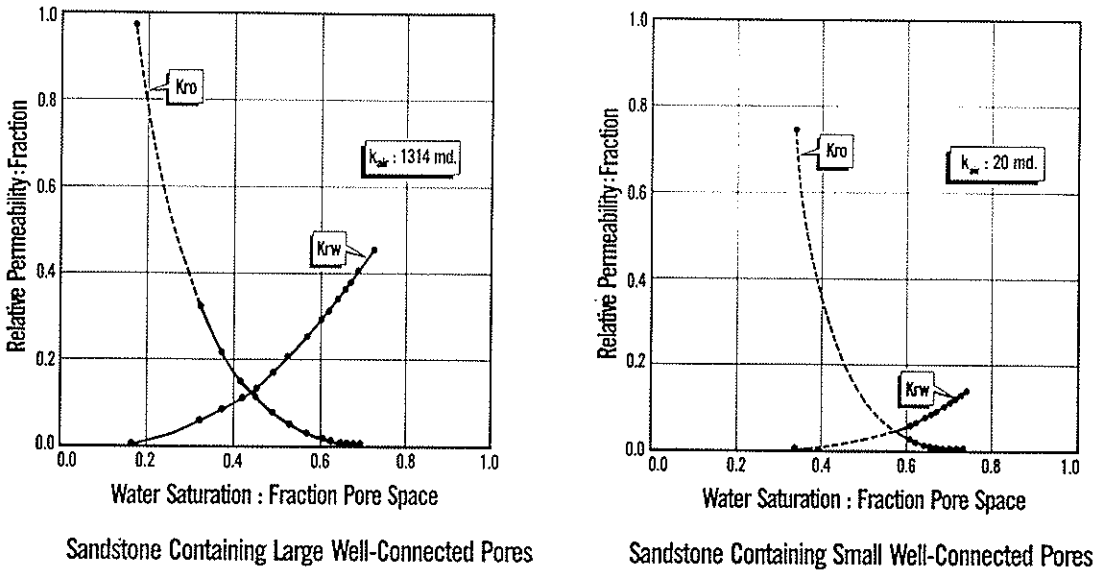

Figure 4.1 *Illustration of two sets of oil and water relative permeability curves plotted as a function of saturation. The left hand figure is typical of a sandstone containing large well-connected pores (with a high air permeability, k_{air}), and the right hand figure is typical of a sandstone containing small well connected pores (with a relatively low air permeability) (from Core Laboratories Course notes).*

Before some relative permeability measurement techniques are described the following section briefly presents a qualitative description of the effect of wettability on relative permeability and phase saturation in a three phase system.

4.0.2 Effect of wettability on relative permeability and phase saturation in a three phase system

The following section (after Gamble 1992) is a brief qualitative description of the effect of wettability on relative permeability and phase saturations in a three phase system (solid and two immiscible liquid phases, where the immiscible phase liquids are taken to be oil and water brine).

Figure 4.2 is a set of schematic diagrams illustrating the effect of contrasting wettability of a rock to a given two-phase system. Let us consider an oil saturated, oil wet, rock forced to imbibe water. In an oil wet rock where oil saturation is high connate water will reside in small discontinuous pore spaces (Figure 4.2.1). With forced imbibition (under pressure) of non-wetting water, oil will still be left coating grains behind the water front, and any oil movement will be by flow across thin films on grain surfaces (Figure 4.2.2). At water breakthrough water permeability rises very rapidly as water channels through larger flow paths, concomitantly, oil continues to drain through thin films coating grains and via oil bridges between grains (Figure 4.2.3). After prolonged flooding a low volume fraction of residual oil is left behind

the swept region as grain coatings, and at this stage water permeability approaches the absolute water permeability of the rock (Figure 4.2.4). After prolonged water flow through oil wet rock the oil residual saturation is relatively low due to the high relative oil permeability. Now let us consider the contrary case of a water wet, oil saturated, rock subject to water imbibition.

In a water wet rock where oil saturation is high connate water resides as pendular rings or grain coatings and the oil occupies the void spaces between grains (Figure 4.2.5). When water flow begins (either by natural imbibition or by forced imbibition) water passes along the water wet grain boundaries and starts to fill the void spaces, in the process oil is trapped by a 'snap-off' mechanism in the pore throats (Figure 4.2.6). Once the water front has passed trapped oil is left as isolated blobs and ganglia in the flow channels, low aspect ratio throat/pore size channels generally do not contain trapped oil (Figure 4.2.7). The trapped oil may considerably impede the flow of water through the rock so that final water permeability may be significantly less than the absolute water permeability of the rock. In addition, it can be seen that residual oil saturation will be enhanced and relative oil permeability greatly reduced with respect to an oil wet rocks.

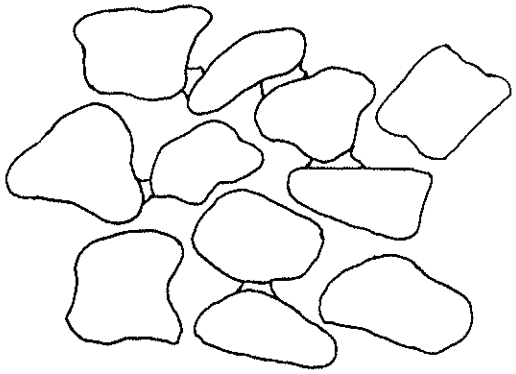

Figure 4.2.1

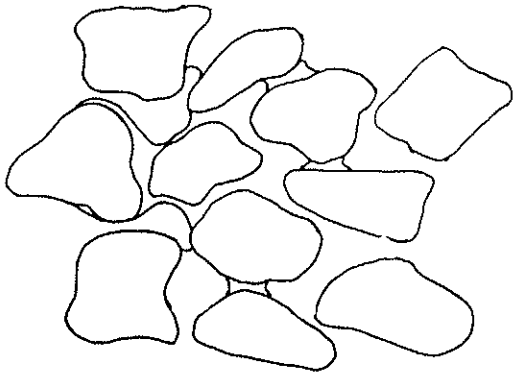

Figure 4.2.2

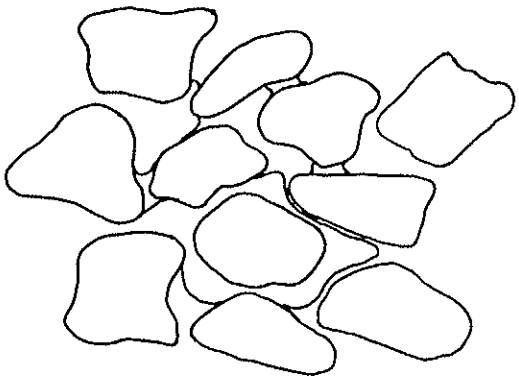

Figure 4.2.3

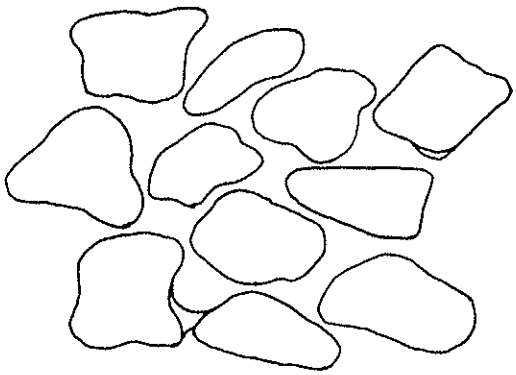

Figure 4.2.4

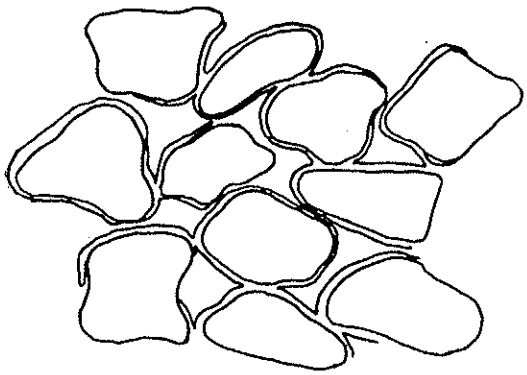

Figure 4.2.5

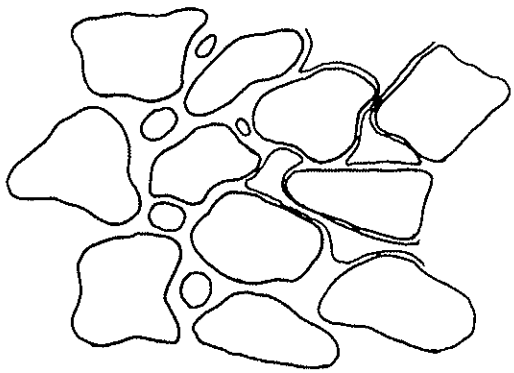

Figure 4.2.6

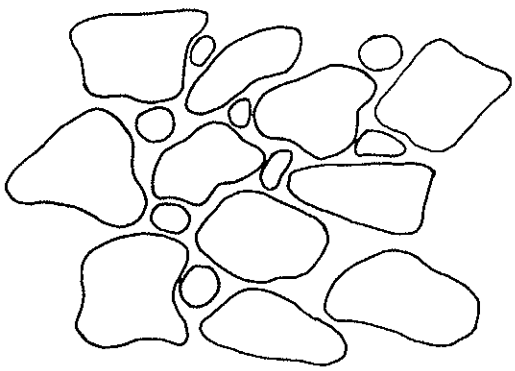

Figure 4.2.7

Figure 4.2 *Graphical illustration of the effect of wettability on the relative permeability and saturation of immiscible phase - brine - aquifer systems, see text for details. Key; rock - yellow, brine - blue and oil - red.*

4.1 Basic waterflood techniques to determine relative permeabilities at residual oil and brine saturations

Basic waterflood tests provide water and oil permeability values (K_w and K_o) at residual water and oil saturations (S_{rw} and S_{ro}) respectively. The tests are usually performed using two phases with a low water/oil viscosity ratio to promote piston like displacement. High viscosity ratios may produce fingering of the water and can lead to poor oil recovery, high residual oil saturations, and poorly constrained residual saturations. Consequently, basic waterflood tests performed on aquifer material saturated with relatively dense non-aqueous phases may prove problematic.

Before a sample is used in a basic waterflood test a standard liquid (brine) resaturation porosity test is performed. At the end of the porosity determination the brine saturated core is flooded with oil until a residual water saturation is obtained (as determined by 'capillary pressure' cell tests). Following this the sample is placed in a core holder and is flushed with oil, the pressure drop across the sample is measured and used to calculate oil permeability (Darcys Law). The sample is then flushed with brine and the evolved oil monitored until no further oil is produced. At this point (ie. at the residual oil saturation) the permeability of the sample to brine is obtained from the newly established pressure drop across the sample. The final brine saturation, determined using the Dean-Stark method, should be consistent with the bulk porosity measurement, the initial residual brine saturation, and the volume of oil evolved during brine flushing. Results of basic water flood tests are commonly plotted as liquid permeability vs brine saturation, a typical plot is shown in Figure 4.3.

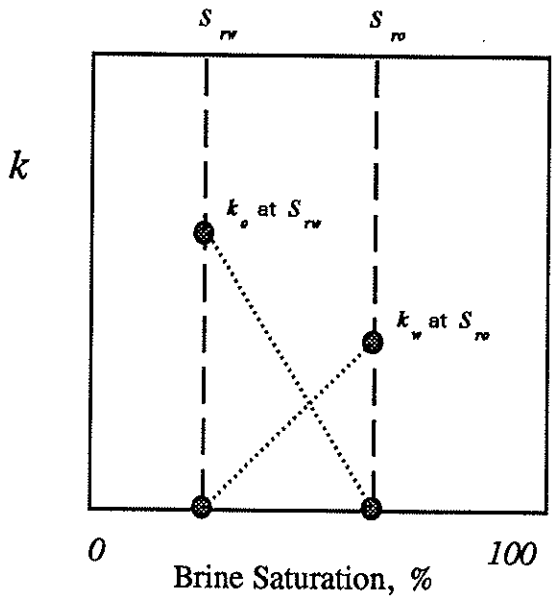

Figure 4.3 *Graphical representation of a typical basic waterflood. Residual oil and water staurations are indicated as are air and brine permeabilities.*

Waterflood susceptibility tests are similar to basic waterflood tests, however, they include incremental data on relative permeability over a range of sample saturations. Two principal techniques are employed steady state and non steady state tests, these are briefly described in the following sections.

4.1.1 Steady state relative permeability tests

The steady-state relative permeability test is schematically illustrated in Figure 4.4. As with a basic water flood test a standard liquid (brine) porosity determination is performed on the sample prior the relative permeability test. The brine saturated core is then placed in a core holder and oil is flushed through the core until a residual brine saturation is obtained. The pressure drop across the core and oil flow rate are used to calculate the permeability of the core to oil (Darcys Law). Oil and water mixtures of varying proportions are then flushed through the core, the final flush being with brine to obtain the permeability of the core to brine at the residual oil saturation. For any given oil-water mixture flushing is continued at a constant flow rate until a constant differential pressure is achieved (typically one to three days).

The respective permeabilities of oil or water for any given oil-water mix is calculated from the pressure drop across the core and the known flow rate of each of the two phases. At each stage of the test saturations are determined from the known sample porosity and the sample weights. It is necessary to remove the sample from the core holder to weigh it at each stage of the test for this reason samples are commonly enclosed in heat shrink wrap or some other tubing to limit errors introduced due to fluid evaporation and/or grain loss. Thorough mixing of the oil/water mixture is provided by mixing heads at each end of the sample (the downstream mixer prevents the two fluids separating which could lead to the wetting phase being drawn back into the core by capillary forces). Commercial laboratories usually obtain steady state data at five saturation points, these include the two end values at the residual water saturation, S_{rw} and at the residual oil saturation, S_{ro}.

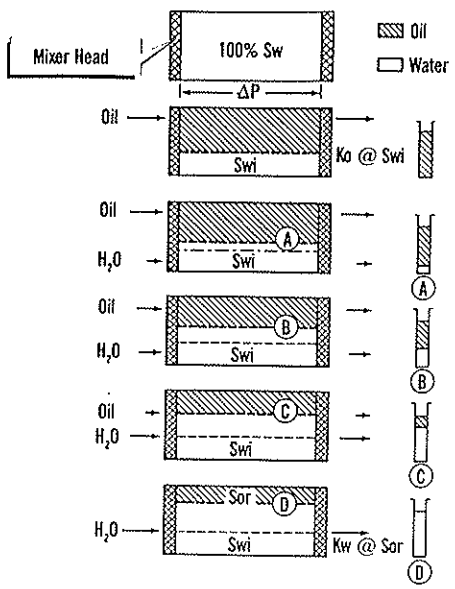

Figure 4.4 *Schematic illustration of a steady state relative permeability test, see text for details (from Core Laboratories course notes).*

4.1.2 Unsteady state relative permeability tests

The unsteady state technique is schematically illustrated in Figure 4.5. As with a basic water flood test a standard liquid (brine) porosity determination is performed on the sample prior to an unsteady state relative permeability test. The brine saturated core is then placed in a core holder and oil is flushed through the sample until water is no longer evolved. At this point oil relative permeability at residual water saturation is obtained from the oil flow rate and the pressure drop across the sample (Darcys Law) and residual water saturation is obtained by weighing the sample. The sample is returned to the core holder and water is then flushed through the core. Oil is initially displaced, however, following water breakthrough both water and oil are evolved. The method is termed unsteady state since saturations of both phases change throughout the water flush. If a constant flow rate is used the pressure drop across the sample will evolve as the proportion of flowing brine increases, and if constant flow pressure is used both phase saturation and flow rate will evolve.

Unsteady state relative permeability tests are usually performed at relatively high flow rates and on short plugs to overcome capillary end effects (no mixer heads are used in this experimental configuration). Consequently, several hundred pore volumes may be injected during the test (this can cause damage and may modify the sample structure). A viscous oil is usually used in the tests to force an early breakthrough, a high viscosity contrast promotes fingering of the water at the oil water interface. This has the effect of prolonging the duration of two phase flow and provides more information for the calculation of the relative permeabilities; a far from trivial task (Johnson, Bossler & Naumann 1959).

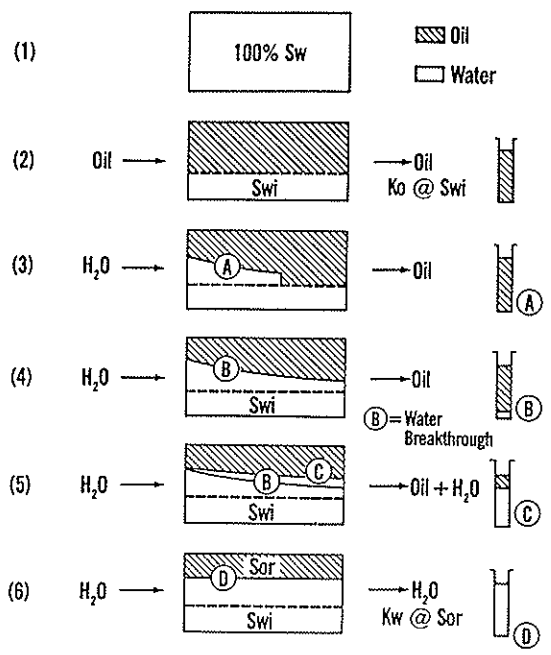

Figure 4.5 *Schematic illustration of an unsteady state relative permeability test, see text for details (from Core Laboratories course notes).*

4.2 Use of centrifuge techniques to obtain relative permeabilities

Centrifuge tests to obtain relative permeabilities are analogous to the unsteady-state waterflood susceptibility tests (eg. Chardaire-Riviere et al. 1992). They are performed in an identical manner to the centrifuge tests performed to obtain 'capillary pressure' curves and require similar data to be recorded.

Unsteady-state tests are limited to studying displacements where the assumptions underlying the Buckley-Leverett theory (see Appendix Section A.3.0) are satisfied (ie. the effects of capillary pressure and gravity are ignored), and only provide relative permeability data over a limited saturation range.

Consequently, to improve the unsteady-state methods, analytical techniques have been developed to take gravity and capillary pressure into account and to obtain relative permeability for the total saturation range. The experimental data require are the pressure drop across a core sample and the cumulative volume of the displaced phase, however, saturation profiles may also be required (obtained by gamma ray attenuation or tomography).

A.1 Definitions used in the study of capillarity

The following sections provide a number of specific definitions to terms used in the study of capillarity.

A.1.1 Surface Tension and Surface Free Energy

The five types of interfaces can be recognised in three phase systems, gas - liquid, gas - solid, liquid -liquid, liquid - solid and solid - solid interfaces.

A general prerequisite for the stable existence of an interface between two phases is that the free energy of the formation of the interface should be positive. The study of capillarity is concerned with interfaces that are sufficiently mobile to assume an equilibrium shape, ie. meniscuses at solid-liquid interfaces, or droplets formed by one liquid in another. Because capillarity deals with equilibrium configurations it is constrained by thermodynamic relationships. Consequently, it can be said to deal with the macroscopic and statistical behaviour of interfaces rather than with the details of their molecular structure.

Surface tension or surface free energy, γ, may be defined as free energy per unit area, but may also be thought of as force per unit length. Two examples are commonly cited in support of these definitions.

The first example, illustrated schematically in Figure A.1.1, shows how surface tension may be considered as a force per unit length. The figure is an illustration of a soap film stretched over a wire frame, one end of which is moveable. Experimentally it can be observed that there is a surface tension force acting on the moveable branch of the frame in the opposite sense to that of the arrow in the figure. If the value of the force per unit length, l, of the branch is denoted by γ, then the work done in moving the branch a distance dx is

$$\text{Work} = \gamma l dx \qquad \text{A.1.1}$$

or

$$\text{Work} = \gamma dA \qquad \text{A.1.2}$$

where $dA = ldx$ and so gives the change in area. The units for the surface tension term, γ, are mN/m.

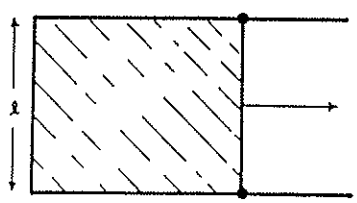

Figure A.1.1 *Schematic illustration of a soap foam over a wire frame one end of which is movable, see text for details (from Adamson 1960).*

The second example commonly used is illustrated in Figure A.2, in this case it illustrates surface tension, or surface free energy, in terms of energy per unit area.

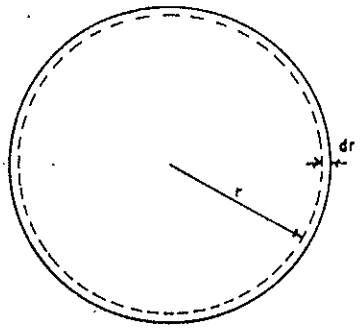

Figure A.1.2 *Scematic illstration of a soap film bubble used in the derivation of surface free energy expressions, see text for details (from Adamson 1960).*

Consider a spherical soap bubble with a radius r. Its total free surface energy is $4\pi r^2\gamma$. If the radius was decreased by dr, then the change in the surface energy would be $8\pi r\gamma dr$. As the bubble shrinks the change in surface energy is balanced by the pressure difference across the soap film, $\Delta\mathbf{P}$. Work against this pressure difference, $\Delta\mathbf{P}4\pi r^2 dr$, is equal to the decrease in surface free energy, ie.

$$\Delta\mathbf{P}4\pi r^2 dr = 8\pi r\gamma dr \qquad \text{A.1.3}$$

or

$$\Delta\mathbf{P} = 2\gamma/r \qquad \text{A.1.4}$$

Eqn A.1.4 predicts that the smaller the bubble the greater the pressure of the air inside as compared to the air outside.

These two examples show that equilibrium surfaces may be treated either by the concept of surface tension, or by the equivalent concept of surface free energy.

Eqn A.1.4 is a special case of a more general relationship that is the basic equation of capillarity, the Young and Laplace equation. In general it is necessary to use two radii of curvature to describe a curved surface (in the case of a sphere these are equal). If the surface is to be in mechanical equilibrium the work done needs to be stated with respect to both radii of curvature, ie.

$$\Delta\mathbf{P} = \gamma(1/R_1 + 1/R_2) \qquad \text{A.1.5}$$

Note that Eqn A.1.5 reduces to A.1.4 when both radii are the same. A special case exists for a plane surface, then the two radii are each infinite and ΔP is therefore zero, consequently there is no pressure difference across the plane.

A.1.2 A simplified model of Capillary Rise based on Surface Free Energy expressions

Capillary rise is often approximated by the Young and Laplace equation (Eqn A.1.5). If we consider a wetting liquid within a capillary (ie. a liquid that makes a contact angle of 0° with the wall), it is constrained to lie within the capillary with a concave shape, see Figure A.1.3. The pressure difference will then be given by Eqn A.1.5, and its sign is such that the pressure in the liquid is less than in the gas phase (note that the radii of curvature always lies on the side of the interface with the greater pressure).

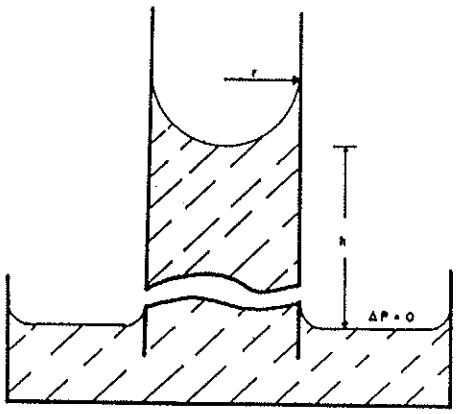

Figure A.1.3 *Schematic illustration of the capillary rise phenomena, see text for details (from Adamson 1960).*

If the capillary is circular in cross-section and not too large in radius, then the meniscus will be approximately hemispherical, the two radii of curvature are equal to each other and Eqn A.1.5 reduces A.1.4 where r is now the radius of the capillary. If h denotes the height of the meniscus above a flat liquid surface (for which $\Delta\mathbf{P}$ must be zero), as illustrated in Figure A.1.3, then $\Delta\mathbf{P}$ in Eqn A.1.4 must equal the hydrostatic pressure drop in the column of liquid in the capillary, ie.

$$\Delta\mathbf{P} = \Delta\rho g h = 2\gamma/r \qquad \text{A.1.6}$$

where $\Delta\rho$ is the difference in density of the liquid and gas phases and g is gravitational acceleration. $\Delta\mathbf{P}$ in the above example may also be referred to as the capillary pressure. Rearranging Eqn A.1.6 a capillary constant, a, can be defined as,

$$a^2 = hr = 2\gamma/\Delta\rho g \qquad \text{A.1.7}$$

If the liquid fails to wet the walls of the capillary, ie. has a contact angle of 180°, the simple treatment above gives the same answer. However, in this case there is now a capillary depression because the meniscus is convex, and h is now the depth of the meniscus depression.

The general case is of a liquid that makes an angle of θ° with the capillary wall, if it is still taken that the meniscus is spherical in shape then it follows from geometric

consideration that $R_2 = r/\cos\theta$ and since $R_1 = R_2$ then Eqn A.1.7 becomes

$$\Delta\rho gh = 2\gamma \cos\theta/r \qquad \text{A.1.8}$$

A.1.3 Contact Angle Phenomena

In many instances a liquid placed on a solid will not wet the solid but remain as a drop having a definite angle of contact between the liquid and solid phases. This situation is illustrated in Figure A.1.4.

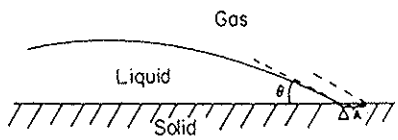

Figure A.1.4 *Illustration of the geometry of a wetting phase-solid contact (from Adamson 1960).*

The change in the surface free energy of the system, ΔG^s, accompanying a small displacement of the liquid, such that there is a change in the area of the solid covered by the liquid, ΔA, is given by

$$\Delta G^s = \Delta A(\gamma_{SL} - \gamma_{SV}) + \Delta A\gamma_{LV} \cos(\theta - \Delta\theta) \qquad \text{A.1.9}$$

where the subscripts SL, SV and LV denote the solid-liquid, solid-vapour and liquid-vapour surfaces respectively.

At equilibrium

$$\lim_{\Delta A \to 0} \Delta G^s/\Delta A = 0 \qquad \text{A.1.10}$$

and

$$\gamma_{SL} - \gamma_{SV} + \gamma_{LV} \cos\theta = 0 \qquad \text{A.1.11}$$

or

$$A_{SLV} = \gamma_{LV} \cos\theta = \gamma_{SV} - \gamma_{SL} \qquad \text{A.1.12}$$

where A_{SLV} is the adhesion tension. Eqn A.1.12 is known as the Young & Dupré equation.

For practical purposes if the contact angle is greater than 90° then the liquid is said not to wet the solid. In this case the liquid may be expected to move about the surface easily and is not expected to enter the capillary pores. In the extreme case where the liquid has a contact angle of zero then Eqn A.1.11 ceases to hold and the imbalance

of free surface energies is now given by a spreading co-efficient, $S_{L/S}$, which can be shown to be given by

$$S_{L/S} = \gamma_{SV} - \gamma_{LV} - \gamma_{SL} \qquad \text{A.1.13}$$

$S_{L/S}$ is positive if spreading is accompanied by a decrease in free energy, ie. the spreading spontaneous.

A.1.4 Wetting as a Contact Phenomena

Wetting and non-wetting are general terms and as Adamson (1960) notes "tend to be defined in terms of the desired effect". However, wetting is usually taken to mean that the contact angle between a liquid and a solid is near zero or so close to zero that a liquid spreads over the solid easily, and non-wetting means that the angle is greater than 90° so that the liquid tends to ball up and run off the surface easily.

With reference to Eqns A.1.11 and A.1.12, if wetting (or spreading) is to occur then γ_{SL} and γ_{LV} should be as small as possible.

A.1.5 Wetting as a Capillary Action Phenomena

Combining Eqns A.1.6 and A.1.8 we obtain

$$\Delta P = 2\gamma_{LV} \cos \theta / r \qquad \text{A.1.14}$$

This expression relates the pressure difference across a meniscus in a capillary, where θ is the angle between the meniscus and the capillary wall, and r is the capillary radius. If θ is not zero then from A.1.11

$$\Delta P = 2(\gamma_{SV} - \gamma_{SL})/r \qquad \text{A.1.15}$$

alternatively if θ is zero then A.1.14 reduces to

$$\Delta P = 2\gamma_{LV}/r \qquad \text{A.1.16}$$

A.1.6 The relationship between Capillary Pressure and Saturation

Capillary pressure can intuitively be related to saturation as described below.

Consider a three phase system consisting of a porous solid, a wetting phase and a non-wetting phase as illustrated in Figure A.1.5.

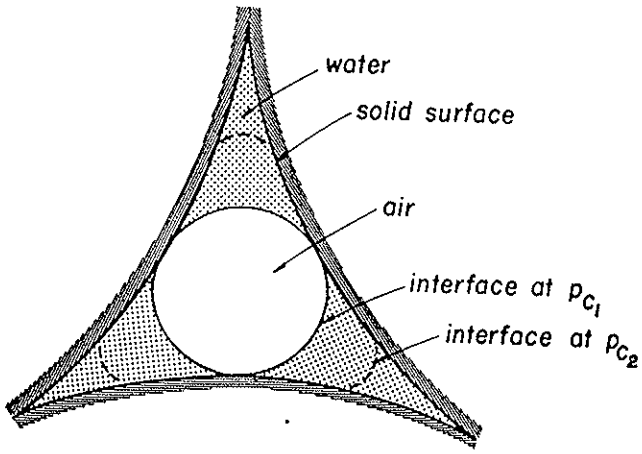

Figure A.1.5 *Scematic illustration of the relationship between saturation and capillary pressure (from Corey 1977).*

The figure illustrates a cross-section of a representative pore space within a body of rock in an equilibrium condition. However, if capillary pressure is increased from p_{c1} to p_{c2}, either by an increase in the non-wetting phase pressure or by a decrease in the wetting phase pressure, then a volume of the wetting phase will be displaced from the pore space. Consequently, the partial saturation of each fluid is a function of capillary pressure, ie.

$$S = \text{fn}(\Delta P) \qquad \text{A.1.17}$$

where S is phase saturation

If the pore space were initially fully occupied with water a finite value of capillary pressure must be exceeded before the non-wetting phase can intrude into the pore volume, this is known as the phase pore entry pressure.

A.2 The centrifuge equation

Figure A.2.1 is a schematic illustration of the geometry of core during a centrifuge test. Where r_1 is the radial distance between the axis of rotation and the inlet end of the sample and r_2 is the radial distance between the axis of rotation and the outlet end of the sample. The following section presents the centrifuge equation (that relates average core saturation, core saturation at the inlet end, and pressure) and a qualitative description of a solution to the equation.

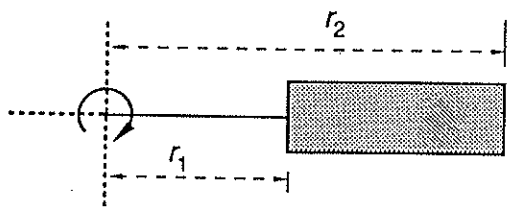

Figure A.2.1 *Illustration of the geometry involved in the derivation of the centrifuge equation.*

A.2.1 A solution to the centrifuge equation

Referring to Figure A.2.1, the capillary pressure at a radius r: $r_1 < r < r_2$ is given by

$$p_c = 0.5\Delta\rho\omega^2(r_2^2 - r^2) \qquad \text{A.2.1}$$

and the capillary pressure at the inlet end at r_1 is

$$p_{c1} = 0.5\Delta\rho\omega^2(r_2^2 - r_1^2) \qquad \text{A.2.2}$$

where ω is the angular frequency (rad/sec) of the centrifuge. The average saturation is defined by

$$\overline{S} = \frac{1}{r_2 - r_1}\int_{r_1}^{r_2} S(r)dr \qquad \text{A.2.3}$$

Substituting p_c from Eqn A.2.1 gives the centrifuge equation that has to be inverted based on measured data;

$$\overline{S}(p_{c1}) = \frac{1+f}{2p_{c1}}\int_0^{p_{c1}} \frac{S(p_c)dp_c}{\sqrt{1-\frac{p_c}{p_{c1}}(1-f^2)}} \qquad \text{A.2.4}$$

where $f = r_1/r_2$, $p_{c1} = p_c(r_1)$ and where $p_{c2} = 0$.

The centrifuge method can also be used to measure negative capillary pressure (during forced imbibition) for wettability determinations. To do this a water wet, oil saturated core, after water has been previously spontaneously imbibed, is placed in an inverted bucket in the centrifuge and more water forced into the core. In this case the form of Eqn A.2.4 is still the same provided the following substitutions are made: $f \rightarrow r_2/r_1$ and $p_{c1} \rightarrow p_{c2}$. Oil is produced at r_1 where $p_{c1} = 0$ and the capillary pressure at p_{c2} is now negative.

Eqn A.2.4 is difficult to use as the integral is unstable. Direct numerical solution methods to the problem are scarce unless data are forced into an assumed functional form of the capillary pressure curve, however, Hermansen et al. (1991) have developed a rapid method of solving the expression without recourse to iterations, numerical differentiation, curve fitting or any assumptions of functional form. Hermansen et al. (1991) were able to show good agreement with 'capillary pressure' curves obtained by porous plate displacement ('capillary pressure' cell method), MICP tests and in the interpretation of synthetic data. The method was also shown to be applicable to the results of forced imbibition (wettability) experiments

(consequently, both wettability index and pore entry pressure data may be obtained from a single test procedure).

A.3 Buckley-Leverett displacement theory

Buckley & Leverett (1942) suggested that the displacement of a front between two immiscible fluids should obey a material balance (over an infinitesimal element, δx, of the system in the direction of unidirectional macroscopic flow),

$$(\delta S_w/\delta t)_x = -(Q_t/\phi A)(\delta F_w/\delta x)_t \qquad \text{A.3.1}$$

where Q_t is the total flow rate through the cross section A, where $F_w = Q_w/Q_t$ (the fraction of the flowing stream comprising displacing fluid), and where ϕ is porosity. Eqn A.3.1 can be recast into the form

$$(\delta x/\delta t)_{Sw} = (Q_t/\phi A)(\delta F_w/\delta S_w)_t \qquad \text{A.3.2}$$

stating that the advance of a plane of fixed saturation, S_w, is proportional to the rate of change in the composition of the flowing stream with saturation.

If F_w is known as a function of S_w and t, time history of saturation profiles could be calculated. By neglecting gravity and capillary forces Buckley & Leverett (1942) estimated F_w by approximating it to the 'fractional flow function' f_w. They defined f_w as

$$f_w = 1 / (1 + (\mu_w K_{ro}/\mu_o K_{rw}) \qquad \text{A.3.3}$$

where μ_w and μ_o are the viscosities of water and oil respectively, and K_{ro} and K_{rw} are water permeabilities at residual oil and residual water saturations respectively. Fractional flow is typically plotted as fractional flow vs saturation (Figure A.3.1). As f_w is not an explicit function of t, Eqn A.3.2 can be integrated to give the position of a particular saturation as a function of time,

$$x_{Sw} = (Q_t t/\phi A)(df_w/dS_w) + x_0 \qquad \text{A.3.4}$$

where x_0 is the position of the water saturation front at $t=0$.

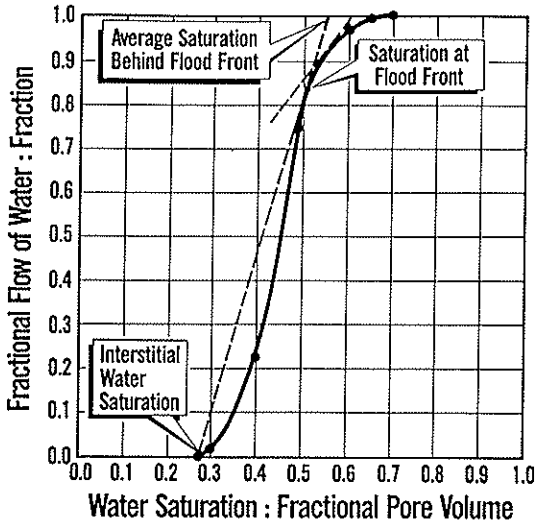

Figure A.3.1 *Illustration of a typical frcational flow-saturation plot, see text for details (from Core Laboratories course notes).*

It is assumed that at $t=0$ the water saturation in the system is uniform. Using Eqn A.3.4 all water saturations can be represented from S_{rw} to $(1\text{-}S_{ro})$. Each saturation front will pass through the system at a rate in direct proportion to $f_w' = df_w/dS_w$, this is illustrated graphically in Figure A.3.1. Commonly fractional flow curves are sigmoidal, the inflection point marking sample saturation at water breakthrough. However, convex upward curve, Figure A.3.2, is a manifestation of piston like displacement (obtained at moderate to high oil viscosities) and a concave downward shape (obtained at low oil viscosities and low water-oil viscosity contrasts), Figure A.3.3, implies that all saturations can be seen to have independent mobility (ie. fingering of water into the oil).

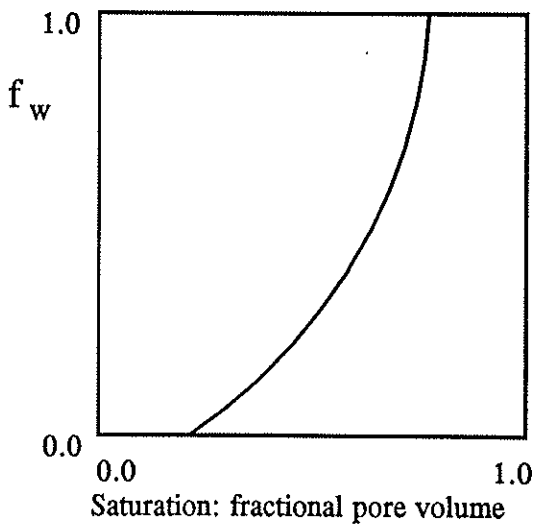

Figure A.3.2 *Schematic illustration of a fractional flow-saturation plot where displacemnet is piston like.*

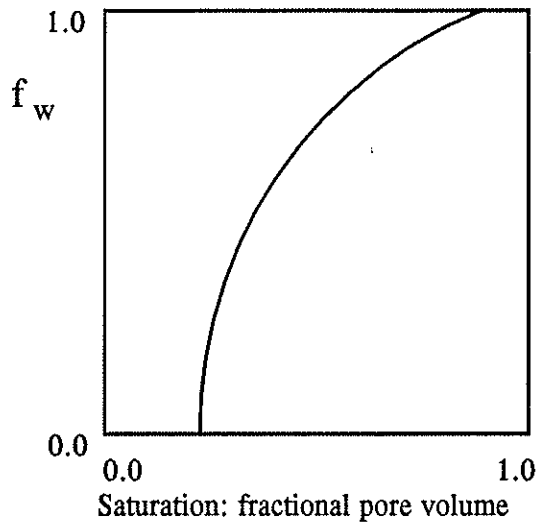

Figure A.3.3 *Schematic illustration of a fractional flow-saturation plot where fingering is occouring and all saturations have independent mobilities.*

References

Adamson, A. W. (1960) Physical chemistry of surfaces. John Wiley & Sons, N.Y.

Bloomfield, J. P., French, L. J. & de La Fourniere, E. (1992) Sellafield 2 Permo-Trias Poro-Perm. Compiled factual report. NIREX/BGS Core Characterisation Report number CC91S/045/CF-A-C (commercial in confidence).

Buckley, S. E. & Leverette, M. C. (1942) Mechanisms of fluid displacement in sands. Trans AIME 146, 107-116

Chardaire-Riviere, C., Chavent, G., Jaffre, J., Liu, J & Bourbiaux, B. J. (1992) Simultaneous estimation of relative permeabilities and capillary pressure. SPEFE, (December 1992), 283-289

Corey, A. T. (1977) Mechanics of heterogeneous fluids in porous media. Water Resources Publications, Colorado.

Dansom, A. W. (1967) Physical chemistry of Surfaces. Interscience Publishers, N.Y.

Donaldson, E. C. (1969) Wettability determination and its effect on recovery efficiency. Soc. Pet. Eng. J., March, 13-20

Gamble, I. J. A. (1992) Laboratory aspects of relative permeability. Lecture notes from a one day seminar on Permeability. Held by the Soc. Prof. Well Log Analysts, Burlington House, 18th May 1992.

Hermansen, H., Eliassen, O., Guo, Y. & Skjaeveland, S. M. (1991) Capillary pressure from centrifuge - a new, direct method. In : Advances in core evaluation II (Edited by Worthington, P. F. and Langeran, D.). Gordon & Breach Science Publishers, Philadelphia. 453-468

Johnson, E. F., Bossler, D. P. & Naumann V O. (1959) Calculation of relative permeability from displacement experiments. Trans AIME, 216, 370-372

Topp, G. C. (1969) Soil-water hysteresis measured in a sandy loam and compared with the hysteretic domain model. Proc. SSSA, 33

White, N. F., Sunada, D. K., Duke, H. R & Corey, A. T. (1972) Boundary effects in desaturation of porous media. Soil Science, 113